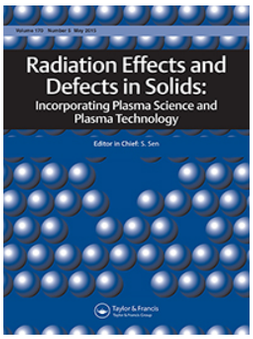

Taylor & Francis
Taylor & Francis Group

Radiation Effects and Defects in Solids
Incorporating Plasma Science and Plasma Technology

ISSN: 1042-0150 (Print) 1029-4953 (Online) Journal homepage: www.tandfonline.com/journals/grad20

The study of gamma irradiation effects on poly (glycolic acid)

Rajeswara Rao Nakka, Venkatappa Rao Thumu, Ramana Reddy SVS & Sanjeeva Rao Buddhiraju

To cite this article: Rajeswara Rao Nakka, Venkatappa Rao Thumu, Ramana Reddy SVS & Sanjeeva Rao Buddhiraju (2015) The study of gamma irradiation effects on poly (glycolic acid), Radiation Effects and Defects in Solids, 170:5, 439-450, DOI: 10.1080/10420150.2015.1036423

To link to this article: https://doi.org/10.1080/10420150.2015.1036423

Radiation Effects & Defects in Solids, 2015
Vol. 170, No. 5, 439–450, http://dx.doi.org/10.1080/10420150.2015.1036423

Taylor & Francis
Taylor & Francis Group

The study of gamma irradiation effects on poly (glycolic acid)

Rajeswara Rao Nakka[a]*, Venkatappa Rao Thumu[a], Ramana Reddy SVS[a] and Sanjeeva Rao Buddhiraju[b]

[a]*Department of Physics, National Institute of Technology, Warangal-506004, India;* [b]*Department of Physics, Government Degree College, Mulugu, Warangal, India*

(*Received 27 February 2014; accepted 13 March 2015*)

We have investigated the effects of gamma irradiation on chemical structure, thermal and morphological properties of biodegradable semi-crystalline poly (glycolic acid) (PGA). PGA samples were subjected to irradiation treatment using a ^{60}Co gamma source with a delivered dose of 30, 60 and 90 kGy, respectively. Gamma irradiation induces cleavage of PGA main chains forming $\sim O\dot{C}H_2$ and $\dot{C}H_2COO\sim$ radicals in both amorphous and crystalline regions. The free radicals formed in the amorphous region abstract atmospheric oxygen and convert them to peroxy radicals. The peroxy radical causes chain scission at the crystal interface through hydrogen abstraction from methylene groups forming the $\sim\dot{C}HCOO\sim$ (I) radical. Consequently, the observed electron spin resonance (ESR) doublet of irradiated PGA is assigned to (I). The disappearance of the ESR signal above 190°C indicates that free radicals are formed in the amorphous region and decay below the melting temperature of PGA. Fourier transform infrared and optical absorption studies confirm that the $\sim O-\overset{O}{\overset{\|}{C}}-O\sim$ groups are not influenced by gamma irradiation. Differential scanning calorimetry (DSC) studies showed that the melting temperature of PGA decreased from 212°C to 202°C upon irradiation. Degree of crystallinity increased initially and then decreased with an increase in radiation as per DSC and X-ray diffraction studies. Irradiation produced changes in the physical properties of PGA as well as affecting the morphology of the material.

Keywords: gamma irradiation; poly (glycolic acid); peroxy radicals; degree of crystallinity; microcracks

1. Introduction

Polymers from renewable resources have drawn increasing attention over the last two decades. Poly (glycolic acid) (PGA) is one among them. PGA is a semi-crystalline polyester exhibiting good mechanical properties, biodegradability, biocompatibility and used in biomedical applications (*1, 2*). Irradiation has been known to alter the properties of polymer through main-chain scission or cross linking (*3, 4*). There has been interest in using gamma radiation to sterilize biomedical devices for medical and veterinary applications (*5*). Therefore, gamma radiation effects on PGA have gained attention. Radioactive degradation results in the rapid fall of molecular weight of PGA. The main mechanism of degradation of the PGA is not only random chain scission but crosslinking also occurs. Large quantities of lower molecular weight units were formed upon irradiation (*6*). The viscosity of PGA slightly decreased and then was found to increase with radiation dose, indicating chain scission and subsequent crosslinking (*7*).

*Corresponding author. Email: rajeshn9@gmail.com

Electron spin resonance (ESR) dosimeters require stable ESR signal with good life time and sensitivity. Alanine is mostly deployed for this function, but it is expensive (*8*). Hence, the search for substitute materials is made. The material should give a sharp ESR line width and be thermally stable at high temperatures. PGA is one of the materials that meets the requirements. In this context, Mejri et al. (*9*) observed an ESR doublet spectrum for gamma-irradiated PGA and assigned the spectrum to be due to the $\sim\dot{C}HCOO\sim$ (I) radical. Though gamma irradiation causes chain scission producing radicals $\sim O\dot{C}H_2$ (II) and $\dot{C}H_2COO\sim$ (III), they have no contribution at room temperature (RT). Annealing experiments were conducted by these authors from 60°C to 140°C to study the fading behavior of free radicals. Stability of free radicals was observed to be more for PGA annealed to 140°C for a period of 35 min, which is ascribed to the semi-crystalline nature of PGA. Thermal stability of free radicals is influenced by the mobility of the polymer chain, particularly in the crystalline and crystalline–amorphous boundary region. The observed decay of free radicals below melting temperature suggests that they are formed in the amorphous region of the polymer.

Identification of free radicals produced in gamma-irradiated PGA is reported by Babanalbandi et al. (*10*) at liquid nitrogen temperature (LNT) (77K) and at RT (300 K). The LNT spectrum is assigned to free radicals (II) and (III) formed due to scission of the polymer backbone and from the elimination of the ester group. The RT spectrum is assigned to $\sim\dot{C}HCOO\sim$ radicals formed by the abstraction of hydrogen from the methylene group located adjacent to the carbonyl group of PGA.

The effect of *in vitro* degradation of PGA scaffolds is reported by Anita et al. (*11*) using scanning electron microscope (SEM), differential scanning calorimeter (DSC) and Fourier transform infrared (FTIR) techniques. The PGA scaffolds are scattered due to the swelling effect of medium absorption. A decrease in melting temperature (T_m) and increase in degree of crystallinity (X_c) of PGA scaffolds were observed. Mechanical properties are found to be reduced. The water molecules easily diffuse into the amorphous region of PGA causing hydrolytic degradation through the cleavage of molecular chains. As a result, the degree of molecular entanglement is decreased promoting higher molecular mobility. The polymer chains realign in a more orderly fashion and facilitate the crystallization process enhancing the degree of crystallinity.

Considering earlier studies, Babanalbandi et al. (*10*) have used the ESR technique to ascertain gamma irradiation effects in PGA and this study was devoted to identification of free radicals. While Merji et al. (*9*) have looked into the dosimetric aspects of PGA using the ESR technique. Radiation-induced changes in crystallinity are reported to be caused by the formation of peroxy radicals (*12*). However, experimental evidence was not provided for the formation of peroxy radicals. According to the reports of Merji et al. (*9*), radicals (II) and (III) do not contribute to the ESR spectrum at RT and the reasons were not explained. Further the stability/kinetics of radicals is related to physical aging. Anita et al. (*11*) have reported *in vitro* degradation and investigated chemical, thermal and morphological properties of PGA scaffolds. However, such studies were not available on gamma irradiation of the PGA. The present work focusses on these aspects.

2. Experimental

2.1. *Materials*

PGA in the form of powder is supplied by *Sigma Aldrich*, Netherlands, with an inherent viscosity of 1.2 dL/g. Samples were subjected to thermal treatment of about 120°C for 8 h prior to the usage. Three packets of PGA sample were prepared for gamma irradiation with different radiation doses, that is, 30, 60 and 90 kGy. Gamma irradiation was performed using Gamma Chamber 900 (GC-900) BRIT, India. The calibrated ^{60}Co based GC-900 with a central dose of

0.15 kGy/h was used in the present study. The uncertainty in doses delivered to samples was ± 5%, so the actual doses are 30 ± 1.5, 60 ± 3 and 90 ± 4.5 kGy. The distribution of radiation dose was nearly uniform and positioned at the center of the chamber using a stand. The total dose given to the sample was controlled by the time of irradiation.

2.2. *Characterization*

2.2.1. *Electron spin resonance*

ESR spectra were recorded on JES-FA200 ESR JOEL spectrometer at an operating frequency of 9.4 GHz (X-band) and 100 kHz modulation at RT. The microwave power was kept at 2.98 mW. The samples were accommodated in quartz tubes with a weight of 5 mg in order to get a quantitative comparison of the ESR intensities under different conditions. The spectrometer was equipped with a variable temperature facility, so that irradiated samples at RT could be annealed to higher temperatures, thus allowing the investigations to study the reactivity of the radicals.

2.2.2. *Fourier transform infrared*

FTIR spectra for the samples in pellet form together with KBr are recorded on a Perkin Elmer spectrometer. Chemical structure of the PGA before and after irradiation is ascertained by monitoring the intensities of absorption bands at various positions.

2.2.3. *UV–visible spectroscopy*

Optical absorption of PGA solutions was recorded on a UV–visible spectrometer (UV-2550; Shimadzu, Kyoto, Japan) in the range of 190–600 nm. Unirradiated and irradiated PGA was dissolved in hexafluoro-2-propanol (*Sigma Aldrich*, USA) with 0.1 mg/mL concentration. Hexafluro-2-propanol was kept as blank.

2.2.4. *Differential scanning calorimeter*

DSC measurements were performed on a DSC-TA Q10 model calorimeter to study the thermal properties of PGA. Approximately 5 mg of samples were sealed into the aluminum crucibles and heated from 50°C to 250°C at a heating rate of 10°C/min in flushing nitrogen gas. The degree of crystallinity of the PGA was calculated by ratioing the melting enthalpy to 139 J/g, the melting enthalpy of 100% crystalline PGA (*13, 14*).

2.2.5. *X-ray diffraction*

The X-ray diffractograms were recorded on a Bruker D8 Advance X-ray diffractometer (XRD). The X-rays were produced using a sealed tube and the wavelength of X-ray was 0.154 nm (Cu Kα). The XRD pattern was recorded in the 2θ range from 10° to 40°, at 0.2° steps and at a fixed counting time of 10 s. The diffracted X-rays were detected using a fast counting detector-based on Silicon strip technology.

2.3. *Scanning electron microscope*

The samples were fixed on a cylindrical microscope stub covered with a carbon strip and the surface of the samples was gold coated using a sputter (Polaron E5200) set at 25 mA for 60 s.

The morphology was then examined under TESCAN VEGA 3 LMU at an accelerating voltage of 5 kV. A magnification of 2000 × was used.

3. Results and discussions

3.1. *Identification and behavior of free radicals: the ESR study*

In general, when polymers are exposed to gamma irradiation, the formation of free radicals takes place. To study the nature of free radicals, ESR spectra are recorded under different conditions, such as radiation dose and temperature.

Dose dependence: For non-irradiated PGA, the ESR signal was not detected, indicating the absence of free radicals. ESR spectra of PGA irradiated to different radiation doses at RT are shown in Figure 1. All PGA samples, regardless of radiation dose produced a similar ESR signal, with an increasing intensity. The spectra are doublets with hyperfine splitting of 2 mT. Gamma irradiation of PGA results in the formation of three types of radicals (*9, 10*). They are $\sim\dot{C}HCOO\sim$ (I), $\sim O\dot{C}H_2$ (II) and $\dot{C}H_2COO\sim$ (III). Radicals (II) and (III) are formed by assuming the cleavage of bond adjacent to ester groups of the PGA main chain, while radical (I) is formed by hydrogen abstraction from a methylene group located adjacent to the carbonyl group of the polymer chain (*13*). As there is one interacting proton, in radical (I), an ESR doublet spectrum is expected. Radical (II) has two interacting alpha protons and gives a triplet spectrum. While radical (III) has no protons in the alpha position, a singlet spectrum is expected but in the case of beta protonic interaction, a triplet spectrum is expected. Since the observed spectrum at RT is a doublet, the presence of radical (I) is expected. The observed increase in intensity of the ESR spectrum with radiation dose suggests that more number of free radicals are formed with an increase in dose. The dose response curve is drawn by plotting the radiation dose against ESR intensity as shown in Figure 2. As expected the radical concentration increases linearly as

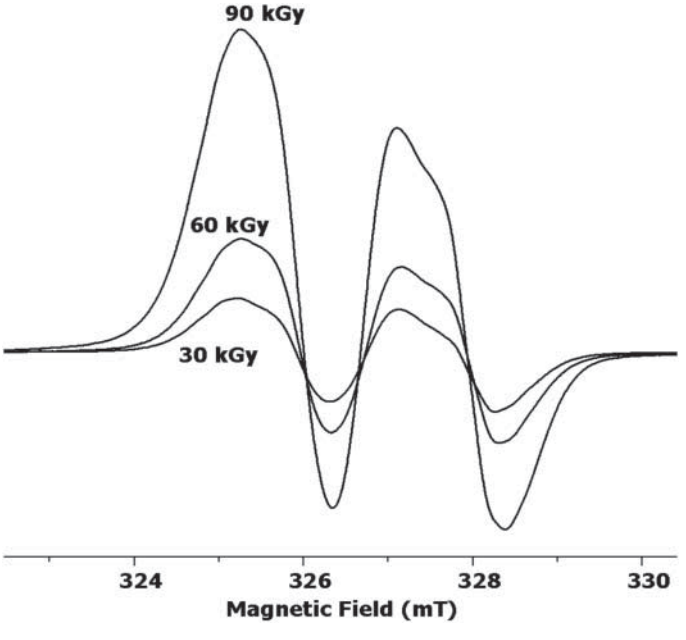

Figure 1. Dose-dependent ESR spectra of PGA irradiated to 30, 60 and 90 kGy.

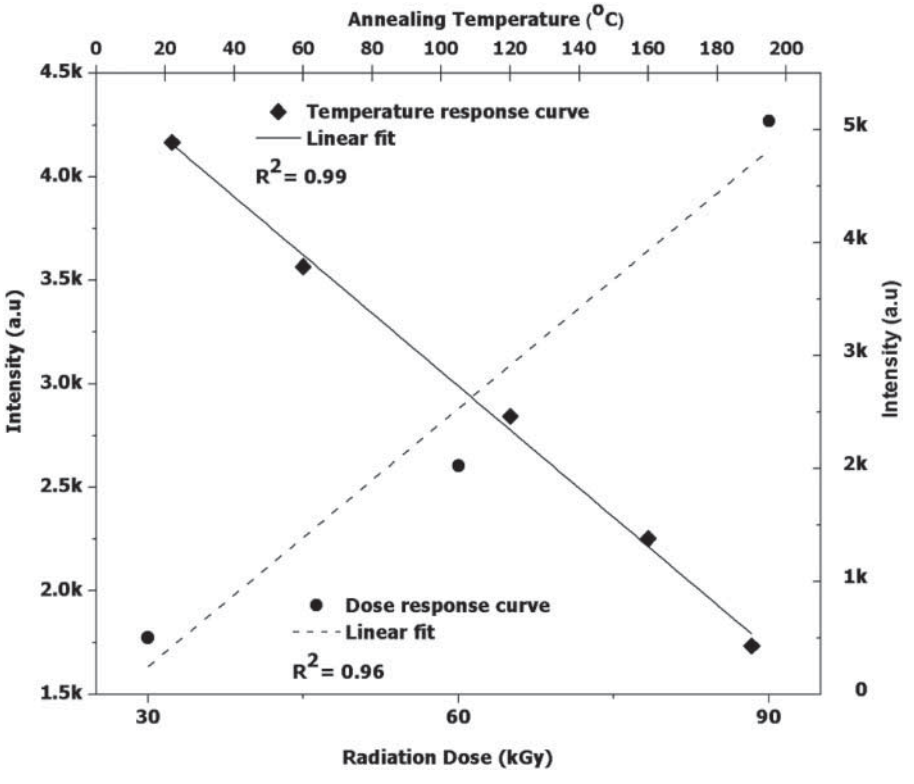

Figure 2. Dose response (•) and temperature response (■) calculated by a linear function.

a function of dose with a regression coefficient (R^2) of 0.96. This linear growth is due to the contribution of radical (I). Merji et al. (*9*) have also observed a linear growth of free radicals in PGA irradiated to low doses (0.1 kGy) and to high doses (300 kGy). They have further reported that growth of radicals in PGA did not reach saturation level even up to a dose of 300 kGy.

Annealing experiments: To assess the thermal stability of free radicals, ESR spectra were recorded at different temperatures as shown in Figure 3. The ESR signal intensity gradually decreases with the increase in temperature. At an annealing temperature of 60°C, a loss of 14.3% free radicals concentration was observed. With the increase in temperature, the loss continues to increase linearly and at 190°C a reduction of 60% was observed. Above 190°C temperature, the ESR signal completely disappeared. The melting temperature (T_m) of PGA is 210°C (*13, 14*). Disappearance of the ESR signal below the melting point suggests that the free radicals are trapped in the amorphous region of the polymer (*9*). Variation of the ESR intensity with temperature is shown in Figure 2. As the ESR spectrum at RT is assigned to radical (I), an increase in temperature causes an increase in thermal energy of radical (I) making it to react or recombine to form stable products. The recombination is optimum at transition temperatures like melting temperature of the polymer (*15*). Therefore, disappearance of radical above 190°C, that is, near the melting temperature of PGA is expected. It further confirms that the free radicals are trapped in the amorphous regions of the polymer. The radical concentration decreases linearly as a function of temperature with a regression coefficient (R^2) of 0.99.

The ESR spectrum of PGA at low doses is an asymmetric doublet whose intensity is not exactly 1:1. The doublet at low dose is simulated to be a superposition of component spectra arising due to radicals (I) and peroxy radicals. Component spectra at low dose are shown in

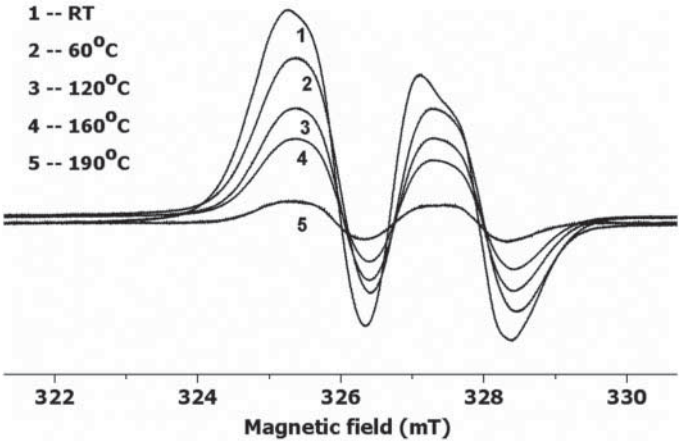

Figure 3. Temperature-dependent ESR spectra of PGA of 90 kGy annealed to 60°C, 120°C, 160°C and 190°C.

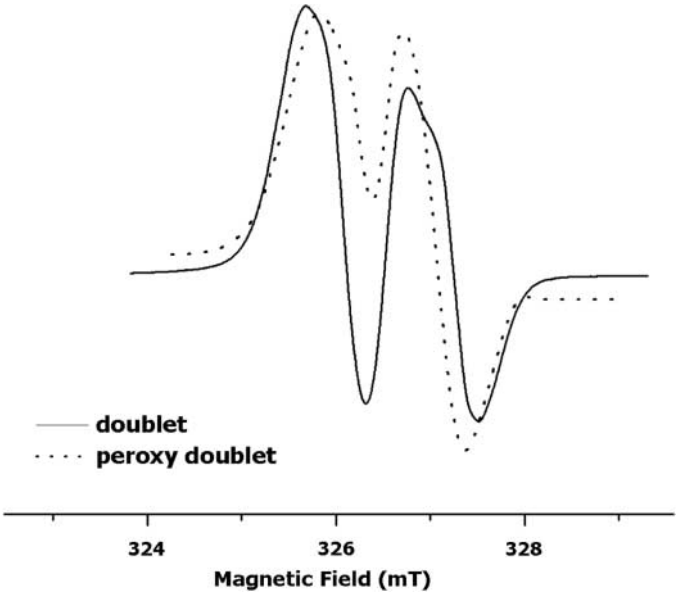

Figure 4. Component spectrum.

Figure 4. Formation of radical (I) is not a direct consequence of gamma irradiation. Instead it is supposed to be formed by abstraction of hydrogen from a methylene group of polymer backbone (*16*). Gamma irradiation of PGA results in backbone scission forming radicals (II) and (III) within both amorphous and crystalline regions. As oxygen diffusion is more in the amorphous region, the free radicals formed in the amorphous region of PGA abstract oxygen and convert them into peroxy radicals (*17*). The peroxy radical in the amorphous region causes chain scission at the crystal interface through hydrogen abstraction from methylene groups and forms $\sim\dot{C}HCOO\sim$ free radicals (*18*).

At higher doses a symmetric doublet spectrum with intensity of 1:1 is observed. Due to the close packing of the crystalline structure, diffusion of oxygen and formation of peroxy radicals is limited. Furthermore, there is a relative increase in probability of crosslinking when compared

with chain scission at a higher dose (*19*). Therefore, the number of chain radicals is more than peroxy radicals at higher doses. Chain radicals are less active in causing the hydrogen abstraction reaction compared with peroxy radicals. The chain radicals have a greater tendency to recombine or crosslink in the crystalline and amorphous region.

3.2. *Chemical characterization: FTIR Studies*

FTIR spectra of unirradiated and irradiated PGA are recorded. Various absorption bands are observed corresponding to different chemical groups of PGA. Prominent among them are (i) the ester carbonyl group at 1744 cm^{-1} (ii) the acetate end group at 1630 cm^{-1} (iii) the C–H group at 1419 cm^{-1} and (iv) the ester C–O group at 1229 cm^{-1} (*20*). Two observations can be made from dose-dependent FTIR measurements. They are (i) major changes in the amplitude of C−O or C–O absorption bands are not observed. In the case of *in vitro* degradation of PGA, diffusion of water into the amorphous phase resulted in hydrolytic degradation through the cleavage of C–O groups. But radiative degradation could not induce cleavage of C–O bond/ C−O bonds. The other observation is (ii) a slight decrease in intensity of 2961 and 1420 cm^{-1} absorption bands is observed as shown in Figure 5. Since these bands are assigned to the C–H moiety, cleavage of these groups is expected. Therefore, FTIR results suggest that the $-C(=O)-O-$ groups are not directly influenced by high-energy radiation.

3.3. *Optical absorption studies: UV–visible spectroscopy*

Optical absorption spectra of unirradiated and irradiated PGA are shown in Figure 6. An absorption band around 280 nm is observed in all cases. As the 280 nm band is assigned to C−O (carbonyl) group (*21*), the presence of these groups is evident in unirradiated and irradiated PGA. Further the peak position and absorption are almost constant, indicating that the $-C(=O)-O-$ groups in PGA are unaffected by gamma irradiation. Therefore, optical absorption measurements support the ESR and FTIR data.

3.4. *Thermal properties: DSC studies*

The DSC thermograms of unirradiated and irradiated PGA are shown in Figure 7. These thermograms demonstrate that structural changes occur in the amorphous and crystalline regions of PGA. The illustrated endothermic peak at 212°C corresponds to melting temperature (T_m) of

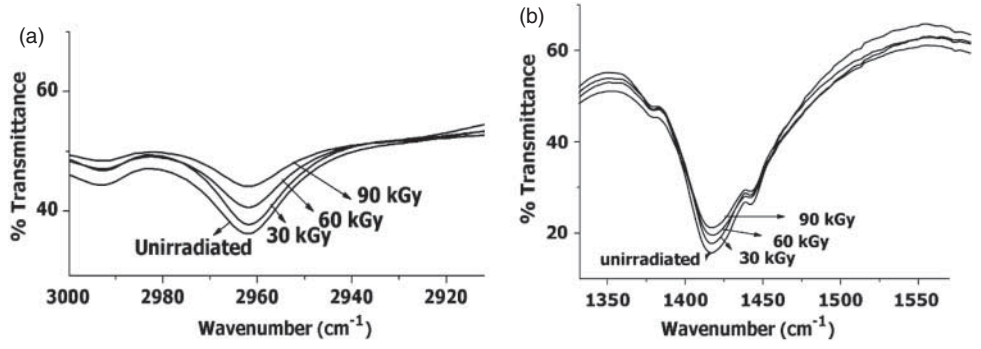

Figure 5. Variation in intensity of absorption bands 2961 cm^{-1} (a) and 1420 cm^{-1} (b) on irradiation on PGA.

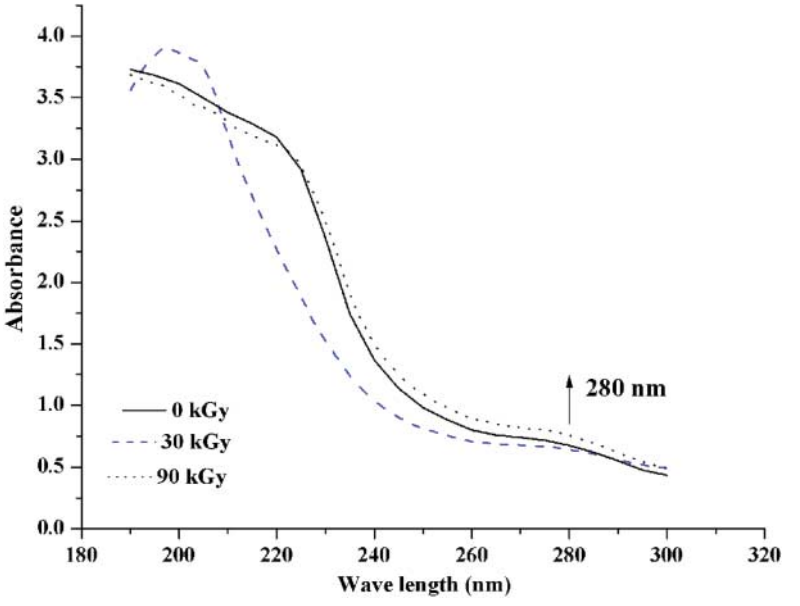

Figure 6. Optical absorption spectra of unirradiated and irradiated PGA solution depicting a small hump at 280 nm wavelength.

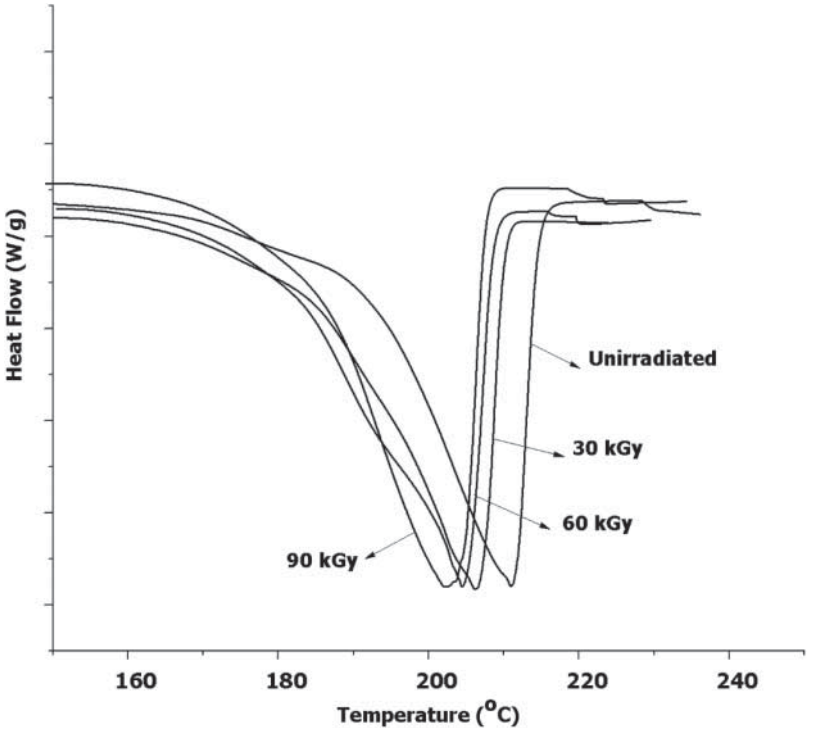

Figure 7. DSC thermograms of unirradiated and irradiated PGA of doses 30, 60 and 90 kGy showing melting transitions.

Table 1. Melting temperatures (T_m), melting enthalpies (ΔH) and degree of crystallinities (X_c) of unirradiated and irradiated PGA.

Radiation dose (kGy)	T°C (T_m)	ΔH J/g	DSC X_c (%)	XRD X_c (%)
0	212	54.89	41.8	39.12
30	207	64.12	46.3	44.06
60	205	56.9	44.3	41.18
90	202	52.1	39.1	37.3

PGA. On irradiation, the melting temperature is found to shift from 212°C to 202°C with radiation dose. Thermal parameters such as melting enthalpy and melting temperatures are listed in Table 1. The data indicate that melting enthalpy and degree of crystallinity (X_c) increase up to 30 kGy dose and are found to subsequently decrease. The decrease of T_m indicates that degradation of PGA occurs in the amorphous region of the polymer where chains are less dense and disordered (*11*). The decrease of T_m also suggests that more number of chains is cleaved resulting in a decrease in molecular weight.

Variation in degree of crystallinity (X_c) against radiation dose is indicated in Figure 8. Due to a main-chain scission of PGA, shorter chains are formed. These fractured chains have better mobility, realign themselves in a more orderly fashion and pack more easily facilitating the crystallization process and causing an increase in degree of crystallinity. The rise in X_c is observed for up to 30 kGy dose beyond which it decreases. Therefore, at higher doses due to extensive chain scission and subsequent radical reaction/radical recombination, X_c decreases. The decrease in X_c is also attributed to deterioration in integrity of crystals beginning from interface to the core of the crystal. The crystalline damage is also evidenced from XRD studies.

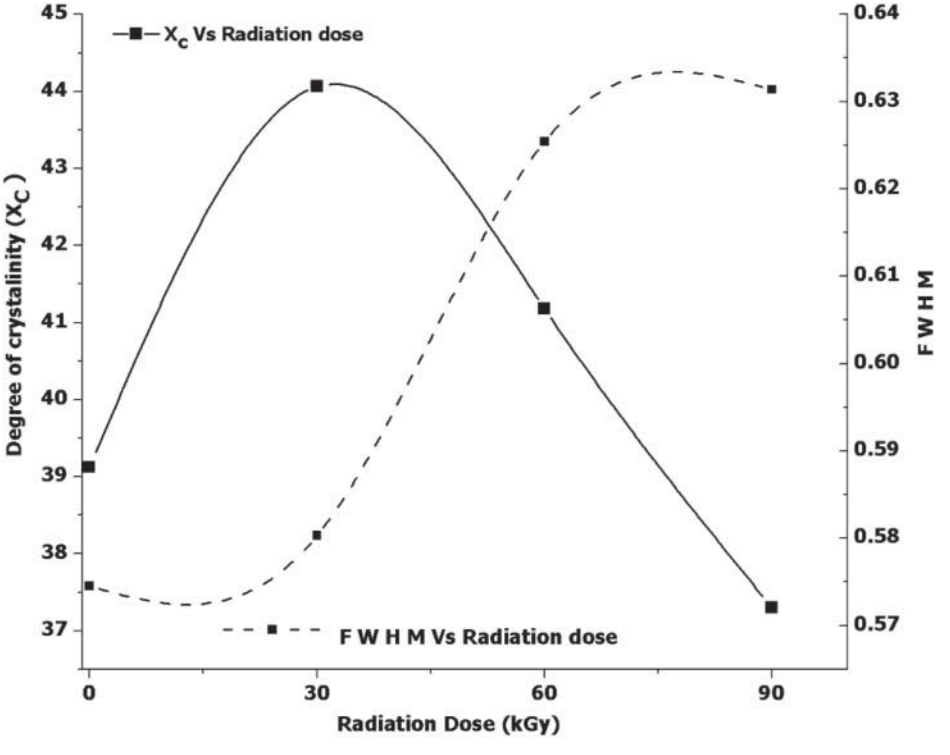

Figure 8. Variation of degree of crystallinity (X_c) and FWHM from XRD diffractograms with radiation dose.

3.5. *Crystallinity properties: XRD studies*

The X-ray diffractogram of unirradiated and irradiated PGA is shown in Figure 9. Two diffraction peaks centered at 2θ equals to 22.18° and 29.01° are observed. The 2θ values correspond to (011) and (200) reflections of PGA (*22, 23*). The unit cell of the PGA is orthorhombic with two molecular chains of glycolic units with fully extended zigzag conformation along the crystallographic direction with a period of 7.16A° (*24*). This planar zigzag chain molecule forms a plane structure parallel to the *c*-axis. The position of diffraction peaks has not changed with radiation dose, indicating that the crystal structure remains the same. However, the degree of crystallinity (X_c) varied with radiation dose as given in Table 1. The X_c is found to increase initially and then decrease with radiation dose similar to DSC measurements. The full-width at half-maximum (FWHM) value is calculated using the Scherrer equation. The increase in FWHM value corresponds to the increase in the distribution of crystallites (*25*). As the distribution of crystallites increases, damage to crystalline integrity is expected. Variation of FWHM with radiation dose is as depicted in Figure 8.

PGA is a semi-crystalline polymer possessing dispersed amorphous as well as the crystalline phase. The PGA with more amorphous content is ideal for drug delivery systems, which require a mono-phase matrix with the homogenous dispersion of active specimen; while PGA with a more crystalline phase and more mechanical retention is desirable for applications as sutures and dental implants. The radiation dose–degree of crystallinity response curve is as shown in Figure 8. The curve indicates that up to a dose of 30 kGy and beyond 60 kGy, the polymer has an amorphous nature, while in the intermediate dose range (30–60 kGy) X_c is high and shows crystalline nature.

3.6. *Microstructures: SEM studies*

SEM micrographs of unirradiated and irradiated PGA are shown in Figure 10. Before irradiation the surface of the PGA is rough as shown in Figure 10(a) corresponding to the porous nature. After irradiation there is an erosion of surface pores. Micro-cracks are observed along the surface

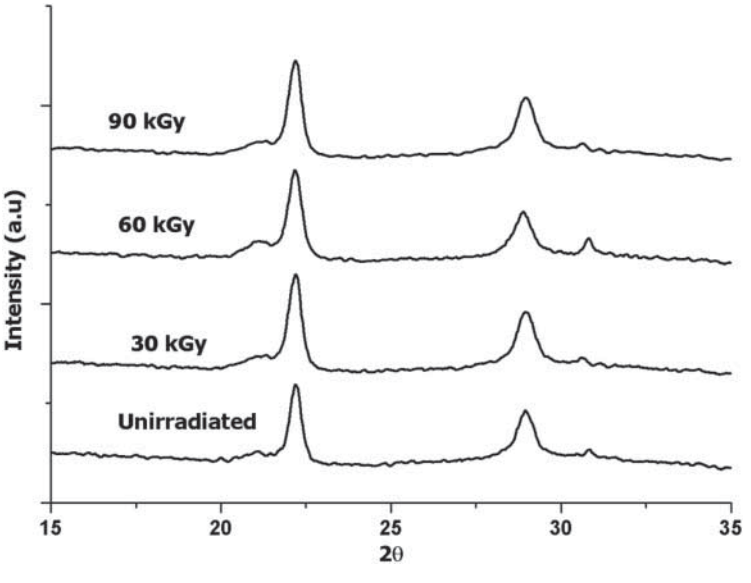

Figure 9. XRD diffractograms of unirradiated and irradiated PGA of radiation doses 30, 60 and 90 kGy.

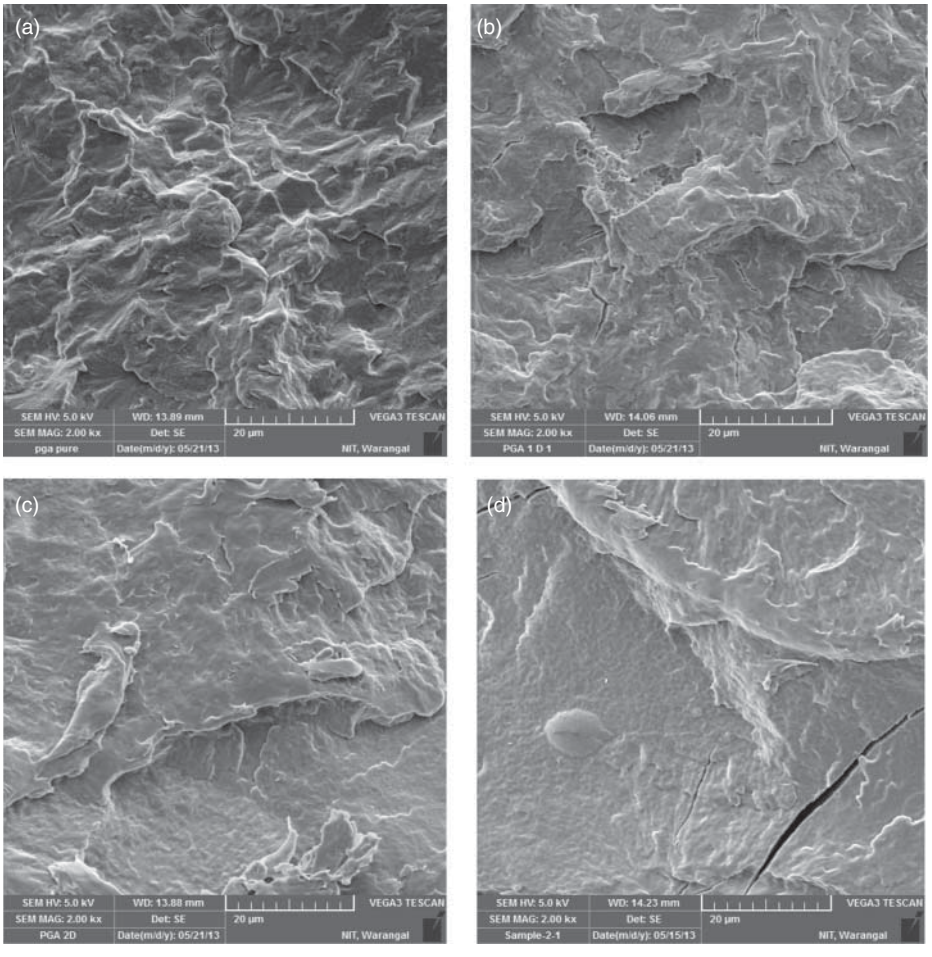

Figure 10. SEM micrographs of unirradiated (a) and irradiated PGA of doses 30 (b), 60 (c) and 90 kGy (d).

and finally the surface becomes smooth at a higher dose as shown in Figure 10(c) and 10(d). The surface defect would be due to the rupture of PGA chains. The micrographs with smooth surface and micro-cracks are indicative of destruction of pores due to radiation.

4. Conclusions

Gamma irradiation causes degradation of PGA through chain scission effecting physical properties such as melting temperature, morphology and crystallinity. We observed the formation of free radicals of type $\sim\dot{C}HCOO$ on gamma irradiation which gives ESR doublet spectrum. Annealing of irradiated PGA to melting temperature results in the disappearance of the ESR signal, indicating that the free radicals are trapped in the amorphous region of the polymer. The cleavage of methylene proton of PGA on irradiation is evidenced by FTIR analysis. Optical absorption measurements indicate that the $\mathrm{coo[\overset{O}{\overset{\|}{C}}\text{-}o\text{-}]}$ groups are not effected by gamma irradiation. DSC studies indicated a decrease in melting temperature of irradiated PGA. Nevertheless, X_c increases at lower doses and then decreases at higher doses. The XRD studies also indicated a similar trend. The studies indicate that up to a dose of 30 kGy and beyond 60 kGy, the polymer has an

amorphous nature and may be suitable for drug delivery applications; while in the intermediate range, 30–60 kGy, the X_c is high and in this dose range the PGA is suitable for applications such as sutures and implants.

Acknowledgements

The authors gratefully acknowledge the UGC-DAE Consortium for Scientific Research, Indore for XRD measurements.

Disclosure statement

No potential conflict of interest was reported by the authors.

References

(1) Ma, P.X.; Langer, R. *Polymers in Medicine and Pharmacy*; Materials Research Society: Pittsburgh, 1995; pp 99–104.
(2) Blake, D.A.; Yolles, S.; Helrich, M.; Cascorbi, H.F.; Eagen, M. *J. Abstract Academy of Pharmaceutical Science Meet*; Springer: San Francisco, CA, 1971.
(3) Chapiro, A. *Radiation Chemistry of Polymeric Systems*; Interscience: London, 1962; pp 353.
(4) Charlesby, A. *Radiation Chemistry Principles, Applications*; VCH: New York, NY, 1987; pp 451.
(5) Athanasiou, K.A.; Niederauer, G.G.; Agrawal, M.G. *Biomaterials*. **1996**, *17*, 93.
(6) Gilding, D.K.; Reed, A.M. *Polymer*. **1979**, *20*, 1459–1464.
(7) Pittman, C.U.; Iqbal, M.; Chen, C.Y.; Helbert, J.N. *J. Poly. Sci: A*. **1978**, *16*, 2721–2724.
(8) Gancheva, V.; Sagstan, E.; Yordanov, N.D. *Rad. Phys. Chem*. **2006**, *75*, 329–335.
(9) Merji, A.; Jelassi, H.; Farah, K.; Hamzaoui, A.H.; Eleuch, H. *World J. Nucl. Sci. Tech*. **2012**, *2*, 73–79.
(10) Babanalbandi, A.; Hill, D.J.T.; O'Donnell, J.H.; Pomery, P.J. *Poly. Degrad. Stab*. **1996**, *52*, 59–66.
(11) Anita, W.T.S.; Arthur, F.T.M. *Poly. Degrad. Stab.* **2003**, *81*, 141–149.
(12) Yeom, B.; Yu, Y.J.; McKellop, H.A.; Salovey, R. *J. Poly. Sci. Part A: Poly. Chem*. **1998**, *36*, 329–339.
(13) Pinkus, A.G.; Subramanyam, R. *J. Poly. Sci: A*. **1984**, *22*, 1131–1140.
(14) Lu, L.; Mikas, A.G. *Polyglycolic Acid Polymer Data Handbook*; Oxford University Press: New York, NY, 1999; pp 566–569.
(15) Bartos, J.; Klimova, M. *Journal of Polymer Science A: Polymer Chemistry*. **1996**, *34*, 1741–1746.
(16) Montanari, L.; Monica, C.; Elena, C.S.; Luisa, V.; Santucci, C.; Monica, B.; Paolo, F. *J. Controlled Release*. **1998**, *56*, 219–229.
(17) Kelen, T. *Oxidative Degradation: Polymer Degradation*; VNR: New York, NY, 1983; pp 107–136.
(18) Loo, J.S.C.; Ooi, C.P.; Boey, F.Y.C. *Biomaterials.* **2005**, *26*, 1359–1367.
(19) Gupta, M.C.; Deshmukh, V.D. *Polymer*. **1983**, *24*, 827–830.
(20) Kister, G.; Cassanas, G.; Vert, M. *Spectrochim. Acta Part A*. **1997**, *53*, 1399–1403.
(21) Rabek Jan, F. *Experimental Methods in Polymer Chemistry*; John Wiley & sons: Bristol, **1980**; pp 211.
(22) Karsten, S.; Epple, M. *Macromol. Chem. Phys*. **1999**, *200*, 2221–2229.
(23) Marega, C.; Marigo, A.; Zannetti, R.; Paganetto, G. *Eur. Poly. J*. **1992**, *28*, 1485–1486.
(24) Chatani, Y.; Kazuakis, S.; Okita, Y.; Hiroyuki, T.; Chuj, K. *Die Makromolekulare Chemie*. **1968,** *113*, 215–229.
(25) Kantoglu, O.; Guven, O. *Nucl. Instrum. Methods B*. **2002**, *197*, 259–264.